THE GEOLOGICAL SOCIETY OF AMERICA®

Optimizing Digital Elevation Model Resolution Inputs and Number of Stream Gauges in Geographic Information System Predictions of Flood Inundation: A Case Study along the Illinois River, USA

ANAS RABIE[1,2]
ERIC PETERSON[3]
JOHN KOSTELNICK[1]
REX ROWLEY[1]

Illinois State University, Department of Geography-Geology, Campus Box 4400, Normal, IL 61790-4400

Key Terms: ***Hydrology, Geographic Information System (GIS), Spatial Analysis, Flood Hazards, River Management***

ABSTRACT

Spatial analysis using Geographic Information Systems (GISs) is evaluated for its ability to predict the potential hazard of a flood event in the Illinois River region in the state of Illinois. The data employed in the analysis are available to the public from trusted organizations such as the Illinois State Geological Survey and the U.S. Geological Survey. Since available GIS data may be limited for flood risk modeling in some parts of the world, the purposes of this study are to examine the use of spatial analysis in a GIS to determine flood inundation risk and to produce an accurate flood inundation vulnerability map employing the least amount of data. This study concentrates on areas that have stream gauge data with definable flood stage(s) and utilizes the inverse distance weighted interpolation method on different digital elevation models (DEMs) with different spatial resolutions (1 m, 10 m, and 30 m) to determine the extent of flooding over the study area. Resulting maps created for the Illinois River region yielded about 80 percent agreement with the effects of an actual flood event on the Illinois River near Peoria, IL, on April 23, 2013. A four-gauge distribution scenario using a 10-m DEM produced the most accurate results, but all scenarios generated reasonable flood simulation. Thus, we speculate that it is possible to create a flood prediction map with a reasonable amount of accuracy using only two initial input data layers: stream gauges and a DEM.

[1]Emails: arabie@kau.edu.sa; jckoste@ilstu.edu; rjrowley@ilstu.edu
[2]Present address: Indiana University, Department of Earth and Atmospheric Sciences, 1001 East 10th Street, Bloomington, IN 47405-1405.
[3] Corresponding author email: ewpeter@ilstu.edu.

INTRODUCTION

Rainfall and runoff gauges are not readily available for every river system, which affects the availability and credibility of hydrological data. Vigorous urbanization of areas coupled with temporal and spatial variation in hydrological characteristics makes the quantitative assessment of runoff characteristics in most areas unattainable (El-Hames and Richards, 1998). Disasters due to natural hazards are subject to many types of uncertainty, which complicates how these disasters are predicted and represented on maps and geovisualizations (Kostelnick et al., 2013). For example, natural variability of streamflow and uncertainty of even "best available" elevation data create ambiguity in defining the floodplain boundary for flood hazard maps.

The term "flood risk" indicates the perceived or actual exposure to loss from a river flooding event during a natural disaster. The level of risk depends on the natural disaster's overall impact on human lives and/or the economy (Safaripour et al., 2012). In order to identify that risk, however, accurate maps showing potential inundation (hazard) are required. Simple maps depicting floodwater distribution allowing real-time and rapid simulations, which can be considered "an effective real-time flood modeling and prediction system" (Al-Sabhan et al., 2003), could give decision makers an understanding of the threatened areas.

For thorough flood modeling to be successful, many models require detailed information, including discharge, precipitation, ambient soil water content, land use, evaporation intensity, watershed infiltration, and the geology and geomorphology of the area. Each of the factors affects the others significantly, and their complex relationship affects the stream runoff. To create an accurate hydrological model, a good grasp of the interaction between such factors is manda-

tory (Kia et al., 2012). However, the limitations of available and reliable data constrain flood modeling in many locations and physical environments around the world. This article postulates that a limited, but critical, set of data may be used in a Geographic Information System (GIS) to generate flood hazard maps with a reasonable level of accuracy. Additionally, we evaluate the use of such data in creating potential inundation scenarios at various scales, or spatial resolutions.

Flood modeling with GIS first requires the selection of suitable input data, including a Digital Elevation Model (DEM) to represent surface topography. DEMs are subject to several potential sources of error and uncertainty, including methods for how elevation values are generated and interpolation methods used to derive a DEM from these elevation values (Fisher and Tate, 2006). Many DEM sources exist today for flood modeling, including those created through Light Detection and Ranging (LiDAR) (typically 1- to 3-m resolution) and those created through other methods (typically 10–30-m resolution or coarser). Resolution will have an effect on point-specific and topographic attributes (Deng et al., 2008). A comparison among the different resolutions of DEMs is necessary to enrich the understanding of any value added given the high expense in acquiring and processing LiDAR data sets (Galzki et al., 2008), especially in parts of the world where LiDAR data are not readily available for flood modeling.

Studies in various environmental applications have found mixed results regarding comparisons of GIS analyses with DEMs at varying spatial resolutions and derived through different elevation sources. For example, Jacoby et al. (2013) concluded that 10-m DEMs were noticeably beneficial for delineating geomorphic features such as cave levels when compared to 30-m DEMs. However, in the context of coastal inundation predictions for sea level rise, Kostelnick et al. (2013) found comparable results in predicted inundation for analyses in coastal Maine for both 10-m and 30-m DEMs from the National Elevation Dataset, which they attributed to similar source elevation data sources for both DEMs (see Gesch [2007]). In another sea level rise inundation study, Gesch (2009) compared four DEMs of varying accuracy and resolution and found significant improvement of predicted inundations derived from DEMs generated from LiDAR compared to those that were not. In contrast, Schroeder et al. (2015) reported no differences in stream profiles generated from 1-m and 3-m DEMs created from the same LiDAR data. An added, and sometimes overlooked, advantage of LiDAR DEMs in the context of hydrologic modeling is their ability to account for features such as levees and drainage canals that may impact predicted inundation extents (Poulter and Halpin, 2008).

The present study provides a demonstration of the viability of creating a flood hazard map using stream gauge spacing and DEMs as the two significant components in determining vulnerability and inundation using a GIS platform. Our primary purpose is to evaluate the minimum amount of data required to produce an accurate GIS model by comparing the accuracy of flood-model results generated from different combinations of stream gauges and DEM resolutions. In other words, we generate several predictive flood models with different DEM and stream gauge input data sources and then systematically reduce and modify input data until the minimum data required to generate an acceptable accuracy level is reached. Validity of the individual models is tested by comparing the predicted flooded areas to actual flooded areas through an accuracy assessment. In short, the approach taken in this study illustrates the development of a methodology for a rapid, easy-to-use, and cost-effective means for implementing flood hazard models. The developed models are practical and can be applied to a wide variety of scenarios for which flood hazards data may be limited.

MATERIALS AND METHODS

Study Area

The study incorporated a portion of the Illinois River, a major tributary of the Mississippi River (Lian et al., 2010), in the State of Illinois (Figure 1). The area was chosen because of the availability of all the needed data, specifically DEMs at different spatial resolutions, a network of stream gauges with predefined flood levels (Table 1), and satellite data for a flood event that inundated the area in spring 2013. The examined segment of the Illinois River has a length approaching 220 km and drainage of roughly 36,350 km^2. Geographically, the study area along the Illinois River extends from Cass and Schuyler Counties in the south to La Salle County in the north. At the southern end of the region, floodplain deposits (alluvium) dominate the bottomlands, with a width ranging from about 5 to 6 km. This belt covers the southern banks of the Illinois River (Worthen, 1868). The southernmost parts are prairies that have thin wood belts skirting the channel. To the north, broken, hilly bluffs run parallel to the river. Humans have heavily modified the Illinois River watershed to support agriculture and urban growth (Akanbi and Singh, 1997). The investigated segment resides in the lower Illinois River, where the floodplain is used for agriculture. To preserve a suitable water depth for ship navigation, seven locks and dams were built on

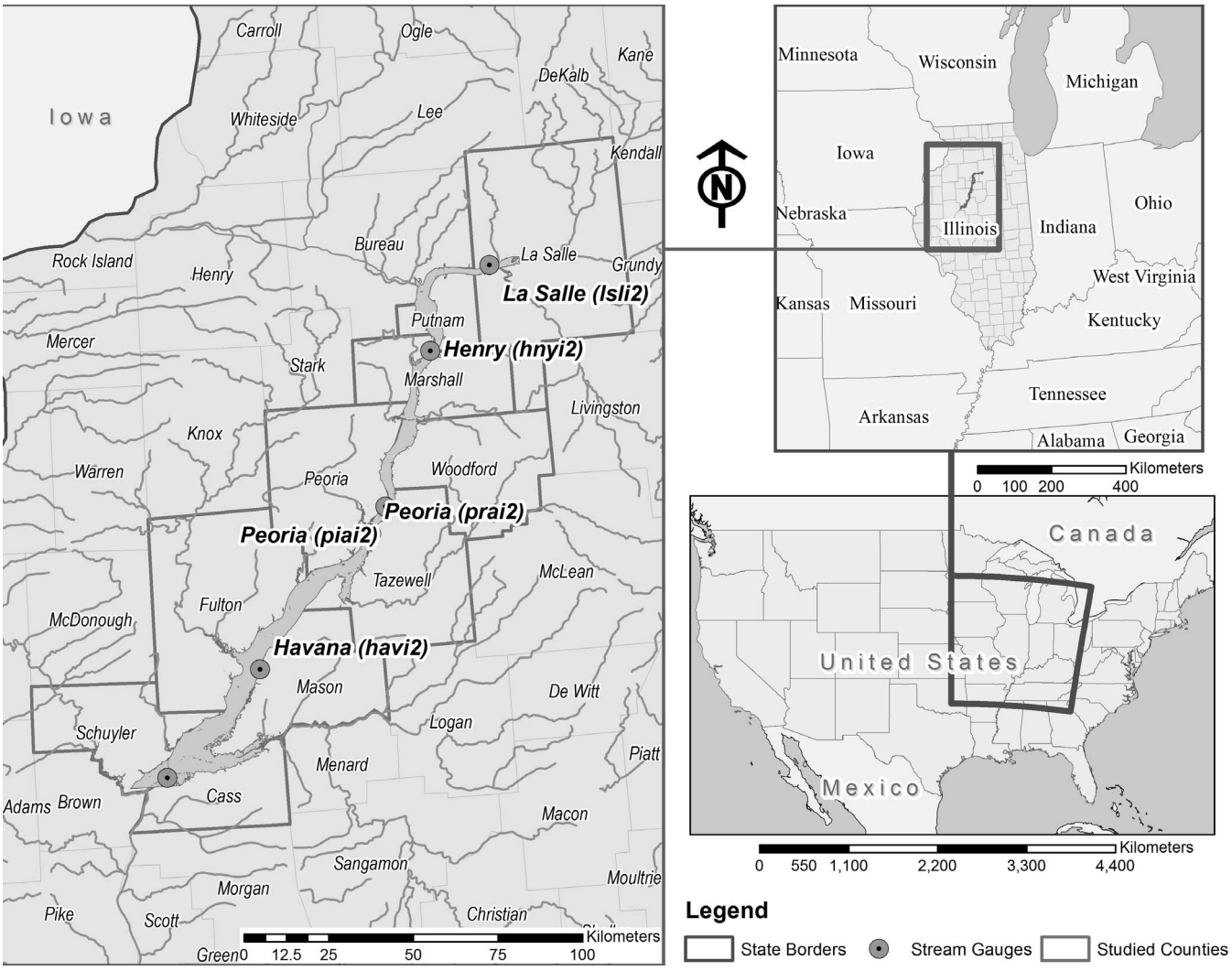

Figure 1. Map of the Illinois River study area showing the stream gauges used in the different distribution scenarios. Map by Anas Rabie.

the Illinois River. Levees and drainage constructions are present that influence the degree of flooding (Lian et al., 2010), which may also have an impact on floodplain modeling.

GIS Data Use

GIS data were collected from different online and no-cost data sources that provided hydrographical,

Table 1. *U.S. Army Corps of Engineers (USACE) and National Weather Service (NWS) stream gauges positioned along the Illinois River and incorporated in this study.*

Station Name	Code	River Mile*	Latitude (°N)	Longitude (°W)	Flood Stage (m.a.s.l.)
Illinois River—LaSalle	lsli2	224.7	41.323611	89.110833	137.2
Illinois River—Henry	hnyi2	196	41.107222	89.356111	136.8
Illinois River—Peoria	piai2	164.6	40.702222	89.564444	136.1
Illinois River—Peoria Lock and Dam	prai2	157.9	40.633333	89.625000	136.2
Illinois River—Havana	havi2	119.6	40.292778	90.068611	133.6
Illinois River—Beardstown	beai2	88.6	40.020278	90.436667	132.5

m.a.s.l. = meters above sea level.
*Miles above the mouth of the Illinois River.

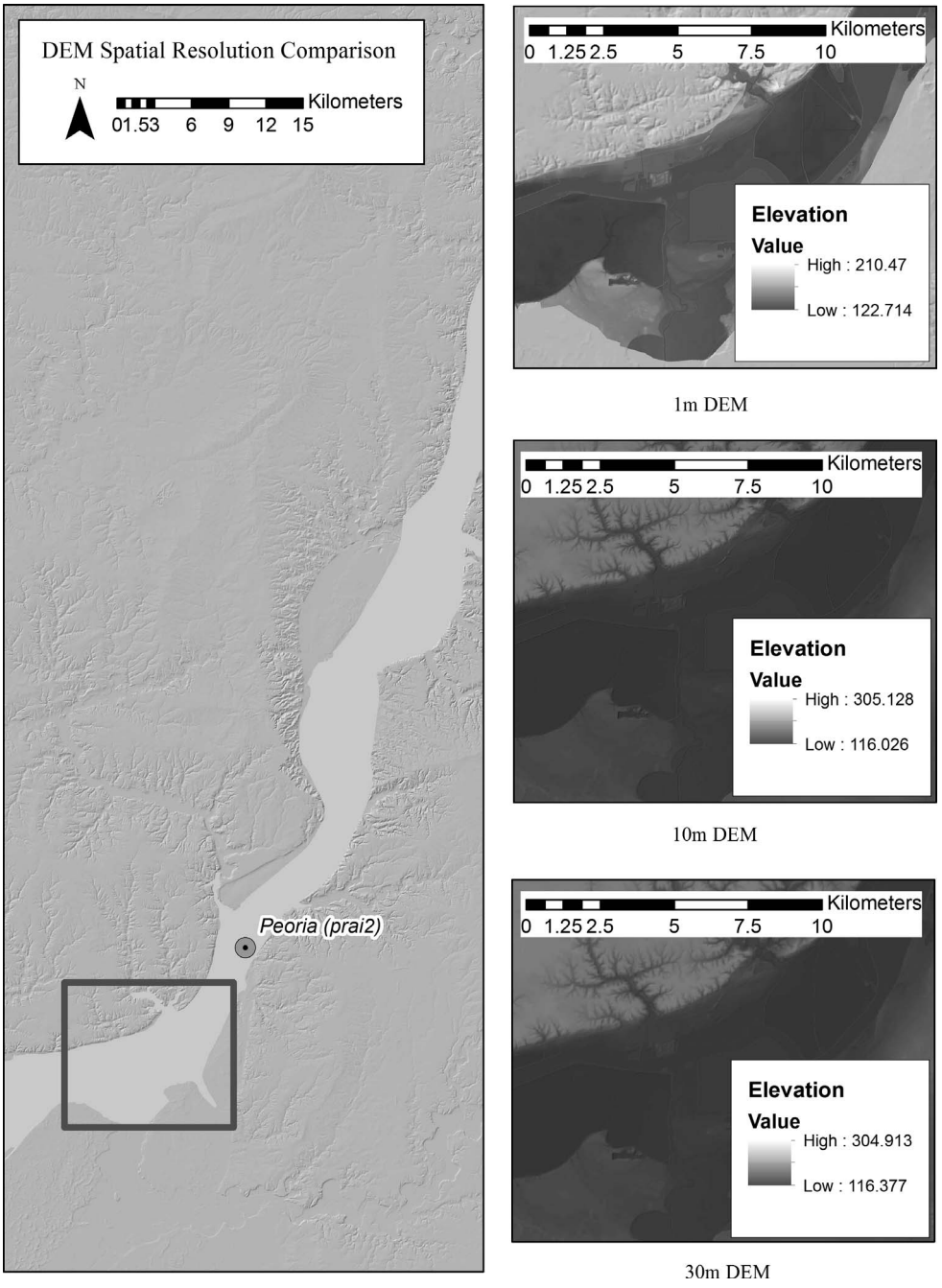

Figure 2. The three DEMs at different spatial resolutions (1 m, 10 m, and 30 m) used in the analysis. The square area highlights the location of the inset DEMs and is presented in Figure 8.

topographical, and related data for the study area. DEMs for the study area were acquired from the U.S. Geological Survey (USGS) National Map Viewer with different resolutions—30 m, 10 m, and 1 m—or with the native resolution of 1 arc second, 1/3 arc second, and 1/9 arc second, respectively. Hydrography data, including polygon water bodies and flow paths as lines, were obtained from the National Hydrography Dataset. Prior to spatially analyzing the data layers, the coordinate systems of the different layers were converted to Universal Transverse Mercator to minimize areal distortion from the map projection for all area calculations. Furthermore, a seamless DEM was created for each of the three different resolutions (Figure 2).

Stream gauges maintained by the U.S. Army Corps of Engineers (USACE) and monitored by the National

Weather Service (NWS) (http://www.weather.gov) provide continuous stage data, along with metadata including longitude and latitude coordinates and flood stage levels for the Illinois River system (Table 1 and Figure 1). Six stream gauges along the Illinois River were incorporated into the study: at La Salle in La Salle County, at Henry in Marshall County, two stream gauges east and southeast of Peoria in Peoria County, at Havana in Mason County, and at Beardstown in Cass County (Table 1).

For the accuracy assessment, Landsat 8 Operational Land Imager (OLI) data were acquired from the USGS Global Visualization Viewer (GLOVIS). Between April 18 and May 16, 2013, the Illinois River experienced a significant flood event (Figure 3). Peak flooding occurred on April 23, but as a result of the 16-day satellite revisit periods, available Landsat imagery tiles were from April 29 for the central and northeastern portions of the study area and from April 20 for the southwestern portion of the study area (Figure 3). Landsat 8 was selected because it provided the only no-cost optical imagery available for the time period of the flood.

Neither of the Landsat 8 image dates is optimal: The April 29 images for the central and northeastern portions of the study area occurred 6 days following the peak event, whereas the April 20 images were occurred 3 days before the flood peak for the southwestern portion (Figure 4). Furthermore, the April 20 images had over 33 percent cloud coverage, which increased error in the image classification. The accuracy assessment model simulated conditions for April 29 using the stage levels provided by NWS for each stream gauge to coincide with the Landsat images of April 29, 2013. This provided uniformity but, of course, restricted our

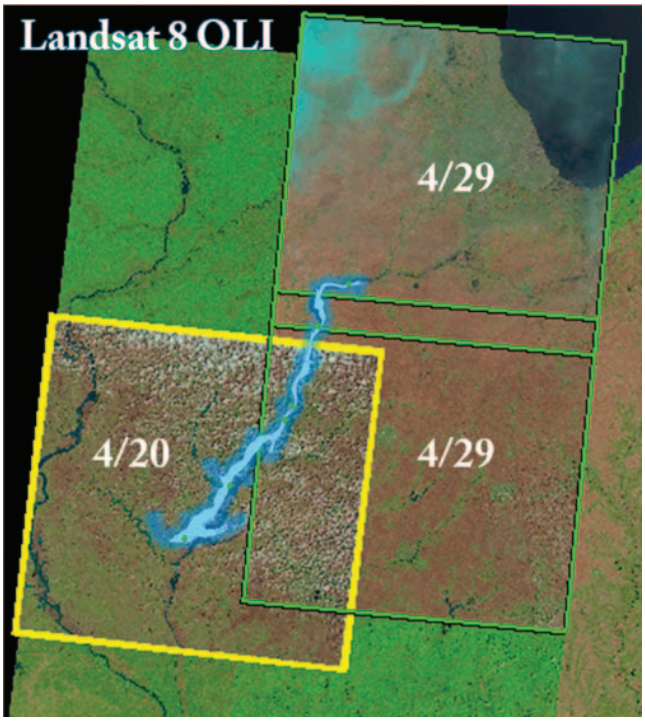

Figure 3. Landsat 8 OLI images as they appear on GLOVIS (February 2014). The study area is shaded in blue.

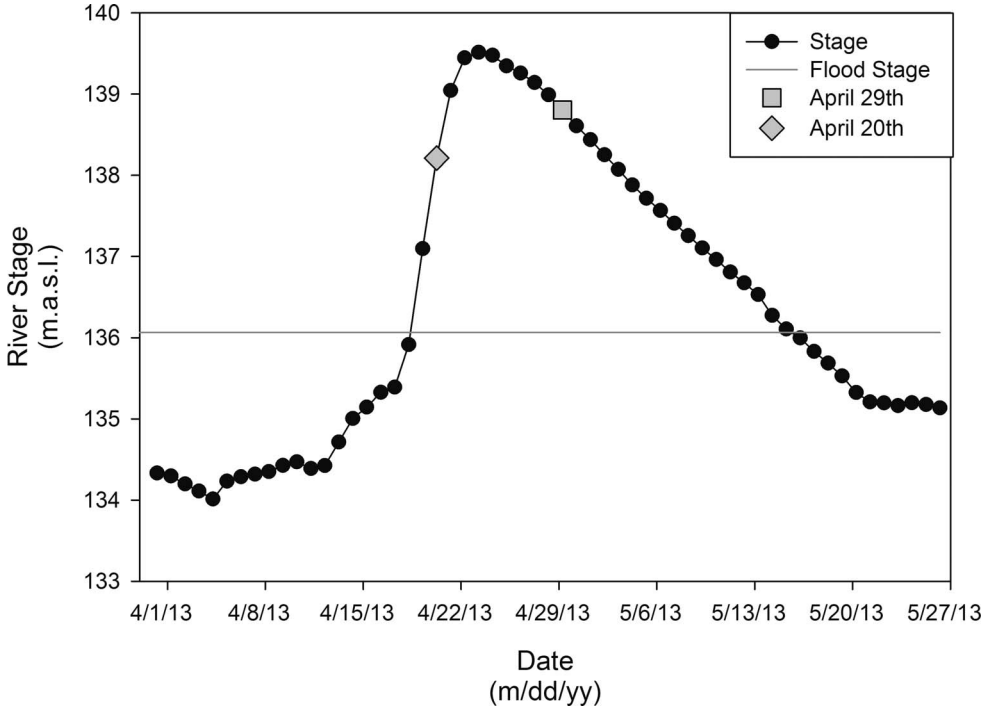

Figure 4. Hydrograph of gauge Peoria (PIAI2). Highlighted dates correspond to the available Landsat imagery. The peak stage drops from 139.14 meters above sea level (m.a.s.l.) on April 23 to 138.99 m.a.s.l. on April 29.

accuracy assessment to only that portion of the study area covered by the April 29 images (see Figure 3). The Landsat 8 OLI imagery, with a spatial resolution of 30 by 30 m (USGS, 2014), was merged into a single image to generate a map of the "actual" flood extent for ground-truthing purposes. The data were classified using a supervised classification approach (where the user creates "training sites" to specify the desired land cover classes) to delineate the locations that were inundated from those that were not inundated. Then, the water associated with the Illinois River, which in this case is defined by the actual water pixels on the day of interest, was isolated from the Landsat reclassified imagery.

The study uses five different stream gauge distributions (Table 2). For each of the five gauge distributions, flood prediction interpolations were generated for the three different DEM resolutions (30 m, 10 m, and 1 m), resulting in a total of 15 different scenarios. The distribution of the stream gauges in each scenario was selected for optimal geographic spacing. For instance, the two–stream gauge distribution used gauges "hnyi2" and "havi2." This decision was made to avoid using the two stream gauges on the edges or the two in the middle that minimize additional errors that may have resulted because of the interpolation process.

Stream-stage data, site name, longitude, and latitude for each gauge station were organized into a table, and five different data sets were created to accommodate the different stream gauge distribution scenarios (Table 2). The data sets were imported into ESRI's ArcGIS and plotted as point locations. The working environment in the GIS model was set so that the results would have the same extent of the Illinois River portion used in this study and to have the same cell size of the desired DEM resolution (30 × 30 m; 10 × 10 m; 1 × 1 m).

Inundation simulations were conducted for the entire study area; however, the accuracy assessment was conducted only on the portion covered by the April 29, 2013, Landsat images.

Simulation Procedure

Figure 5 presents a flow chart of procedures used in this study. A series of raster-based GIS analyses were used to predict areas affected by a flood informed by stream gauge data. Potential inundation surfaces were interpolated for each DEM resolution from the stream stage data using an inverse distance weighted (IDW) technique. The IDW interpolation determines raster cell values using a linearly weighted combination of a set of sample points. IDW interpolation is based upon an assumption that the modeled variable loses influence with distance from data locations (Watson and Philip, 1985). IDW was used to predict water levels at a particular flood stage between gauge locations along the river.

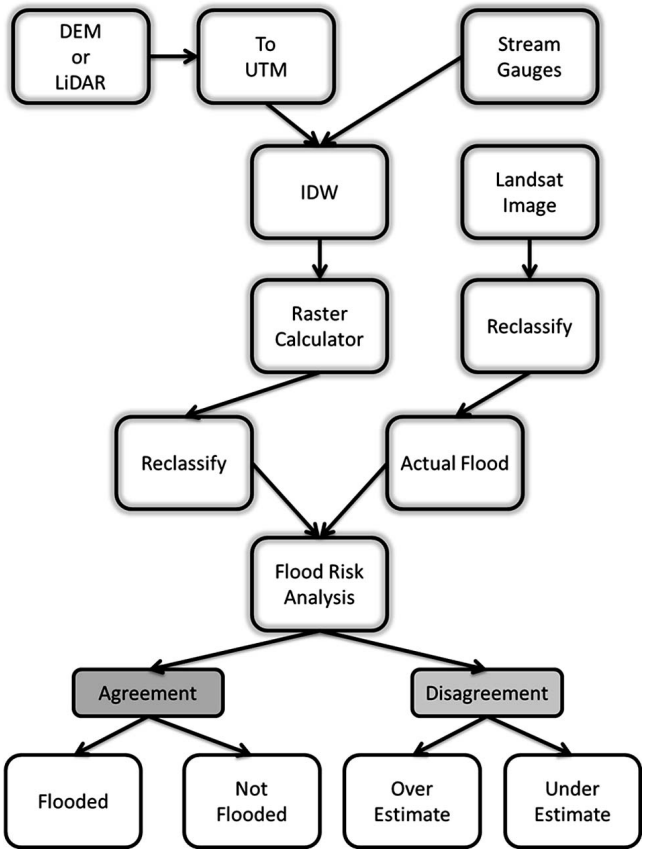

Figure 5. Flow chart of the methodology used to develop the flood hazard model.

Table 2. *Breakdown of stream gauges used for the different distribution scenarios.*

Scenario	La Salle lsli2	Henry hnyi2	Peoria piai2	Peoria Lock and Dam prai2	Havana havi2	Beardstown beai2
6-Gauge	X	X	X	X	X	X
5-Gauge	X	X		X	X	X
4-Gauge	X	X		X		X
3-Gauge	X			X		X
2-Gauge		X			X	

Table 3. *Flood hazard simulation results.*

Landsat Imagery		Simulation Prediction			
Condition	Score	Condition	Score	Calculated Score	Result
Not flooded	0	Not flooded	0	0	Agreement
Not flooded	0	Flooded	1	1	Overestimation
Flooded	10	Not flooded	0	10	Underestimation
Flooded	10	Flooded	1	11	Agreement

The Map Algebra Raster Calculator tool in ArcGIS was used to predict inundation at the different DEM resolutions with the different stream gauge distributions. This was done using an expression that subtracts the IDW results from the desired DEM, providing a flood prediction based on the stream gauge information where any positive value is "Flooded" and any negative value is "Not Flooded." To make the raster calculator results easier to compare visually, the results were reclassified using the Spatial Analyst Reclassify tool.

Generating Comparable Results

An accuracy assessment of the projected inundation from the DEM was performed by comparing results to the actual flood extents, as extracted from Landsat images using ERDAS IMAGINE Supervised Image Classification, based on over 40 training sites on each image. Areas defined as water were designated the numerical score of "10" and those with no water were assigned the score of "0" (Table 3). The results of the simulation prediction were also reclassified into two groups. "Not Flooded" areas were assigned the score of "0" and "Flooded" areas a score of "1."

The two layers were evaluated to determine the agreement in areas designated "Flooded" and "Not Flooded" from the different DEM resolutions by using an expression that simply added the pixel scores of the two reclassifications. The new calculated values indicate either agreement between the simulation and the Landsat image classification (a pixel value of either 11 or 0 reflecting a match between predicted and actual flooding or not, respectively) or a disagreement (values of either 1 or 10 reflecting a mismatch between predicted and actual flooding or not, respectively) (Table 3).

RESULTS

Fifteen flood scenarios were generated, allowing for the comparison of actual flooded areas to those predicted to be inundated on April 29, 2013, for three DEM resolutions and five stream gauge spacings. For each scenario, we computed areas and percentages associated with agreement (flooded and not flooded, in both actual and predicted) and disagreements (overestimation and underestimation) (Table 4). Each of the 15 scenarios exhibited flood inundation agreement over 70 percent of the area simulated.

While the two–stream gauge scenarios produce the lowest overestimation error, at nearly 9 percent for all DEM resolution, the scenarios consistently produced the highest total error (between 29.5 and 29.7 percent, depending on resolution) because of much larger underestimation errors compared to those associated with other stream gauge scenarios (all DEM resolutions around 21 percent) (Figure 6). Scenarios with three, four, five, and six gauges all reported largely similar total error percentages between 22 and 23 percent, depending on DEM resolution, each with relatively consistent over- and underestimation errors (Table 4 and Figure 7). Locations farther from the employed gauges had higher error than did areas near the used gauges, a function of the imperfections in the spatial interpolation process. For every scenario, the area of disagreement for underestimation of potential flood was greater than the area for overestimation (Table 4 and Figure 7b and c).

DISCUSSION

Underestimation or Overestimation

In planning flood mitigation and resiliency measures, it is, of course, crucial to have accurate models available. When such accuracy may not be possible as a result of lack of data or data precision, then an overestimation of hazard may be preferable to an underestimate. It is true that overestimations may prompt planners to believe that some mitigation measures will be cost-effective when they may be unnecessary, but in general the costs of under-preparedness are much higher than being over-prepared, especially when dealing with the consequences of avoidable events (Rosner et al., 2014). The stream gauge scenarios with more than two gauges generated the highest overestimation and the lowest underestimation consistently among the different

Table 4. *Flood hazard simulation disagreements (in km^2) and error percentages, with best models highlighted in bold. Total area of the study location is 610.62 km^2.*

	Overestimate		Underestimate			
Number of Gauges*	km^2	%	km^2	%	Total Disagreement (km^2)	Total Error (%)
DEM resolution, 30 m						
2	53.42	**8.75**	127.92	20.95	181.36	29.70
3	58.83	9.63	78.97	12.93	137.80	22.57
4	58.84	9.64	76.75	**12.57**	135.60	**22.21**
5	58.28	9.54	80.80	13.23	139.08	22.78
6	58.24	9.53	82.33	13.48	140.57	23.02
DEM resolution, 10 m						
2	53.21	**8.72**	126.63	20.74	179.84	29.45
3	58.61	9.59	76.19	12.47	134.81	22.08
4	58.64	9.60	74.08	**12.13**	132.71	**21.73**
5	58.07	9.51	78.02	12.77	136.09	22.29
6	58.06	9.50	79.44	13.01	137.51	22.52
DEM resolution, 1 m						
2	53.32	**8.73**	126.65	20.74	179.98	29.47
3	58.73	9.61	76.24	12.49	134.99	22.11
4	58.75	9.62	74.13	**12.14**	132.89	**21.76**
5	58.20	9.53	78.04	12.78	136.24	22.31
6	58.19	9.53	79.46	13.01	137.66	22.54

DEM = Digital Elevation Model.
*See Table 2 for distribution of gauges.

DEM comparisons, with the four-gauge scenario yielding slightly lower error (Figure 7b). We hypothesize that such a result may be connected to the locations and/or the distances between those stream gauges in the combination of stream gauges used in that scenario. One possibility for the four–stream gauge density scenario yielding lower error is that the IDW interpolation method used in the study area's settings has a threshold that was reached with four gauges, and the results do not necessarily improve with more gauges.

Visual comparison of the extent of the predicted floods (Figure 6) and the error data (Table 4) suggests that no apparent difference exists between the different stream gauge distributions or with use of different DEM resolutions. Underestimation is seen across the edges of the river, whereas overestimation is clustered in the southwest end as well as the northeast end of the Illinois River, which may represent edge effect error.

Although error estimations across the DEM resolutions were relatively consistent, a closer examination of the role of DEM resolution reveals a larger difference between the 30-m DEM and 10-m DEM resolutions than between the 10-m and 1-m DEM resolutions (Figures 7b and 7c). The results are similar to those reported by Jacoby et al. (2013) in that the 10-m DEM generated lower error and was more accurate than were 30-m DEMs for modeling cave entrances. While the use of the 10-m DEM consistently generated models with marginally lower error than those derived from the 1-m DEM, the individual differences among the various gauge distribution scenarios were too small to have significance in terms of the results. A simple quantitative comparison between the results of 10-m DEM models and 1-m DEM models shows that the average difference in this point-to-point comparison is an area of 0.16 km^2, or only 0.03 percent. Generally, higher resolution data provide better sampling and improve the elevation delineations (Hammer et al., 1995; Zhang et al., 1999). However, the differences between 1-m DEMs and more coarse DEMs has not always led to improved accuracy in the models here. For example, Schroeder et al. (2015) found that streambed elevations generated from 1-m and 3-m DEMs were alike.

For this work, the difference between 10-m and 1-m DEM–generated models is found in a release note provided by the USGS regarding the National Elevation Dataset (NED). The NED metadata states that the study area extent is within the Missouri and Mississippi River Basin flood project for the USACE for the Upper Midwest and Plains States, which lasted from 1997 to 2001, using 1/9 arc second (3-m) NED. Later on, the 3-m LiDAR DEMs were used to create the 10-m and 1-m DEM resolutions (Gesch et al., 2002). The re-sampling explains why the results between the two DEM resolutions were comparable to each other: they are derived from the same elevation source. Hence,

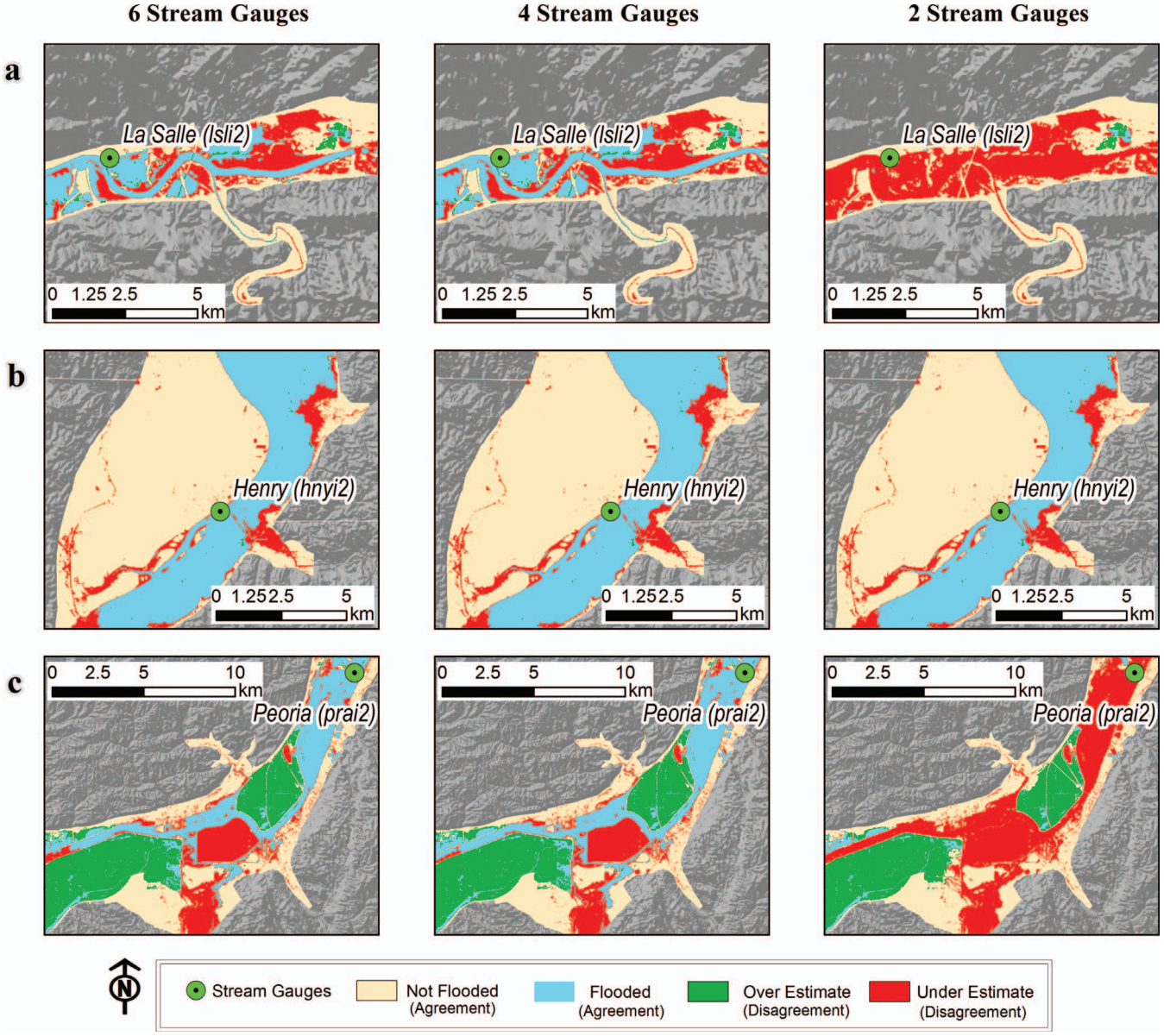

Figure 6. Flood hazard simulation map for the 10-m DEM and selected stream gauge scenarios, where (a) shows the results at La Salle, (b) shows the results at Henry, and (c) shows the results at Peoria Lock and Dam. Refer to Figure 1 for stream gauge locations. Maps by Anas Rabie.

these results suggest that the source elevation data may be more important than merely the spatial resolution of the DEM. Alternatively, two different versions of standard 30-m DEM modules are available in the United States: "Level 1" and "Level 2." The 30-m DEM used in this study is a "Level 1" 30-m DEM, which was derived from 7.5 U.S. Topo maps, also created by the USGS. "Level 2" 30-m DEMs are derived from 1/3 arc second DEMs, which are usually 10-m DEMs. This different elevation source explains, at least in part, why the 30-m DEM used in this study yielded results different from the other DEM resolutions. However, the difference between the 10-m DEM and the 1-m DEM simulations is not significant (Table 3). Our results do not prioritize the choice of DEM resolution to employ when generating inundation maps in areas with similar characteristics to the study locale. Despite the fact that the 30-m DEM data are not as accurate as the LiDAR-derived 10-m and 1-m DEM data, the differences in predicted flood areas among the resolutions is small. Considering the cost of acquiring LiDAR data and the longer processing times required for the larger file sizes

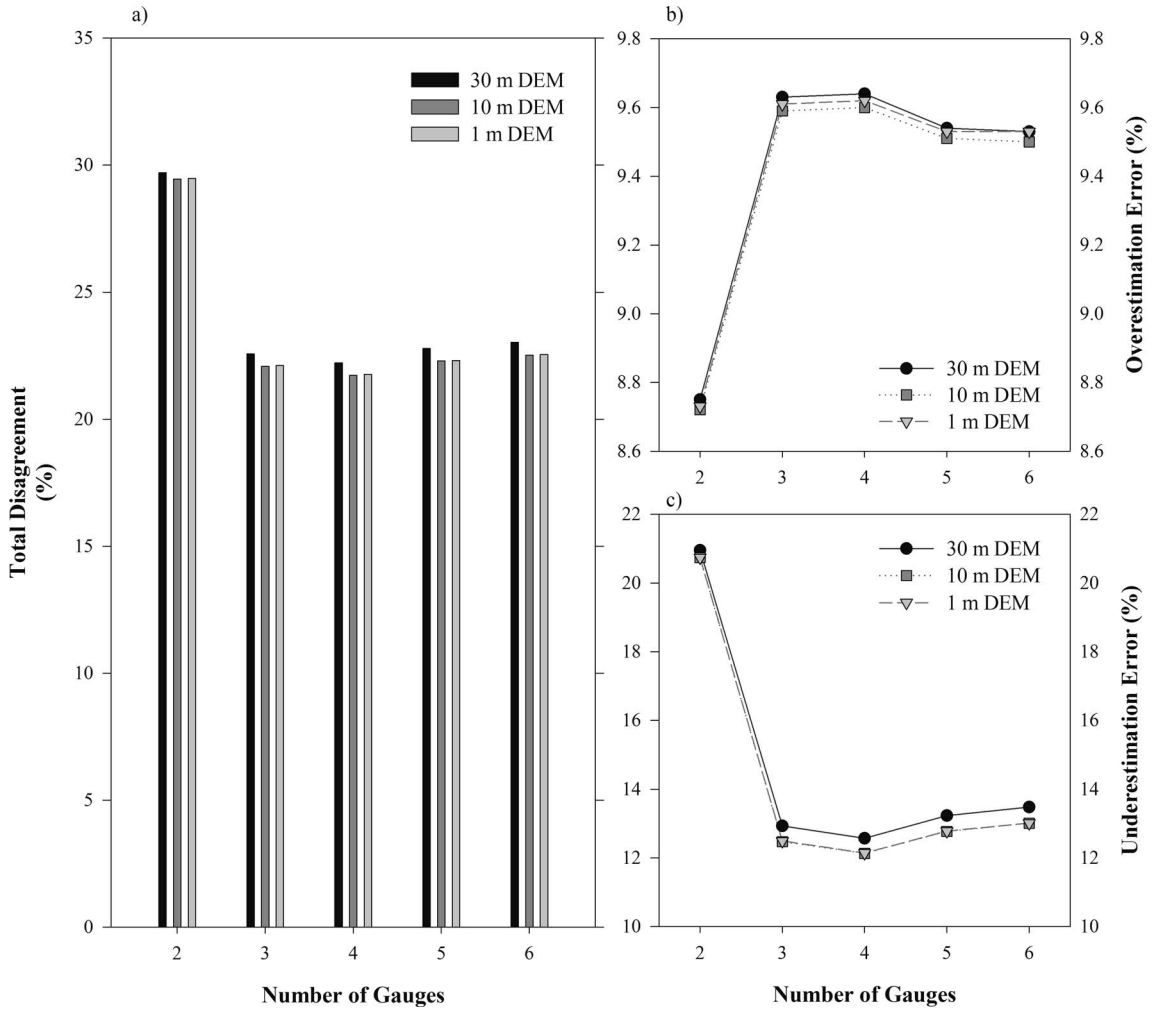

Figure 7. (a) Total disagreement, in percent, for the various stream gauge scenarios for all 15 gauge scenarios. (b) Overestimation and (c) underestimation in the simulated flood hazard errors for the 30-m DEM (black circle), 10-m DEM (dark gray square), and 1-m DEM (light gray triangle).

(5 minutes for 30-m, 12.5 minutes for 10-m, and 38.5 minutes for 1-m DEMs in this study), the results from this study suggest that the 10-m DEM resolution is the preferred resolution for the generation of the inundation maps. The 10-m DEM models produced less error than did the 30-m DEM in one-third the processing time of the 1-m DEM. Given that the model output and error analyses show the 1-m and the 10-m results are very similar, the spatial resolution is not a significant control if the source elevation data (LiDAR) are the same for both DEMs, as is the case in the study in hand, or for an area with similar characteristics to those of the study area. Thus, this work supports the conclusion by Galzki et al. (2008) that lower resolution DEMs are preferred over the 1-m DEM as a result of the computational requirements and lack of availability of data in some areas.

Focus on Disagreement

It is important to realize that the model in this study simulated the flood based solely on elevation and does not examine the role of human influences on water flow dynamics. Human modification of the land surface resulted in major areas of disagreement between observed conditions and modeled conditions in this study (Figure 8). To better show such differences, two elevation profiles were created. Profile A-A′ (Figure 9) is for the agricultural fields within the flood plain, whereas Profile B-B′ (Figure 10) is for a reservoir. Along Profile A-A′, the green areas that represent overestimations are actually agricultural fields protected by levees. This area would be overestimated even at base flow because the stage of the river would be higher than the land elevation. Similarly, along Profile B-B′, the elevation

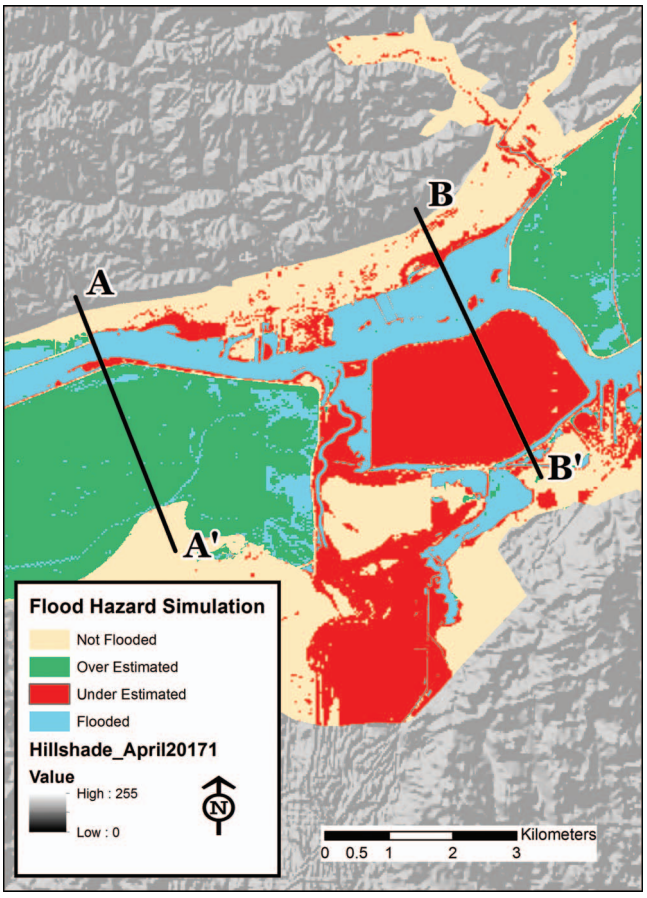

Figure 8. Map showing an example of the total disagreement associated with human modification of nature. Lines A-A′ and B-B′ show the location of the elevation profiles used for the agricultural fields and the reservoir, respectively. Map by Anas Rabie.

of the reservoir perimeter is designed to contain water at an elevation higher than the stage of the river. The models simulated that flood water will not inundate the reservoir, but the reservoir area always appears to be flooded. For both of these locations, the errors are related to human influences, which modify, mask, or alter

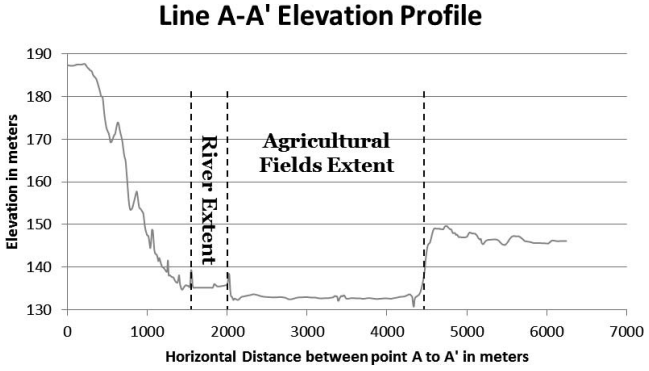

Figure 9. Line A-A′ elevation profile with the extent of river and agricultural fields.

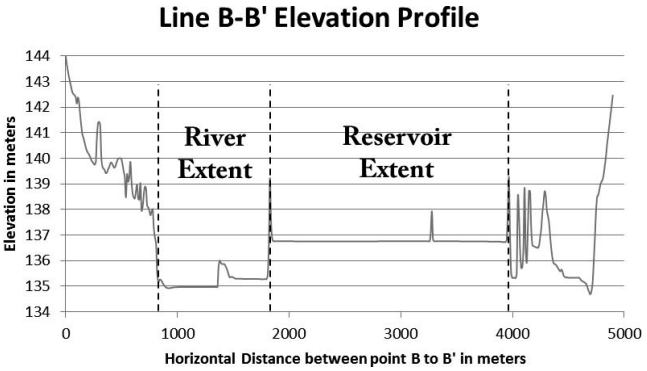

Figure 10. Line B-B′ elevation profile with the extent of river and the reservoir.

the natural conditions. Detailed modeling and vetting can overcome these errors but is beyond the scope of this work. It is, however, important to recognize that hazard mitigation studies on floodplains must take into account such human modification of the landscape that may not be discernable in topography-based simulation of inundation.

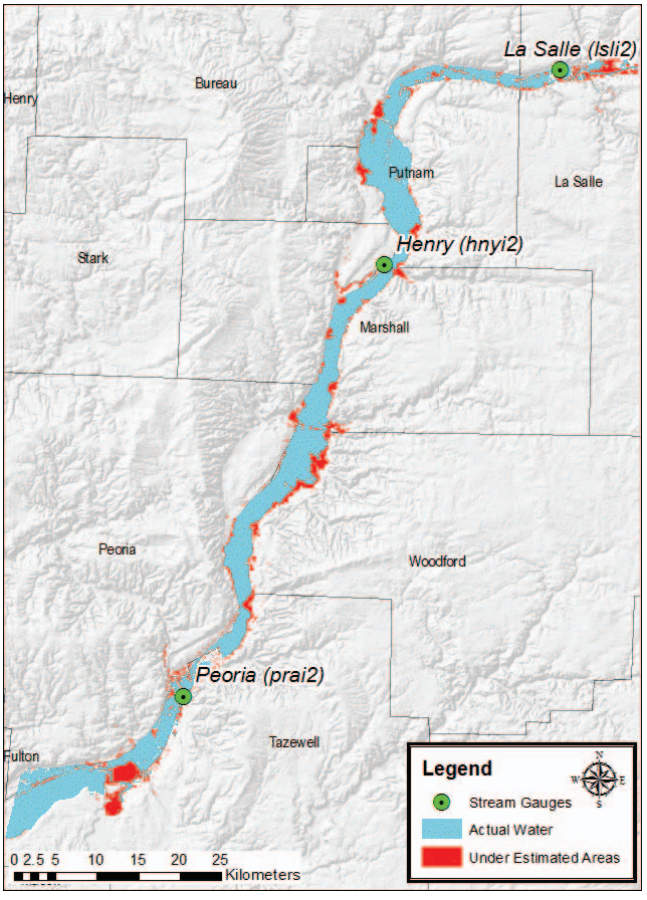

Figure 11. Underestimation map for the four–stream gauge scenario, 10-m DEM resolution. To provide spatial detail of the results, the fourth gauge (bea12) is not shown (off map). Refer to Figure 1 for stream gauge locations. Map by Anas Rabie.

To validate the methods used in this study, Landsat imagery was acquired, but could not be used to represent the actual water distribution on the day of the flood peak in the City of Peoria (April 23, 2013) since that day coincided with heavy rain and severe weather conditions, with clouds covering the extent of the imagery, making it unusable for ground condition assessment. Thus, a later date, April 29, was chosen to represent the peak inundation even though the stage was about 0.8 m below the peak flood (Figure 4). This could explain some of the underestimation in the simulation. In other words, areas predicted as "not flooded" that were actually flooded may be a result of residual flooding on April 29 associated with the peak conditions on April 23. Another possible explanation for the high underestimation is because the land still appears wet following the peak conditions, thus being classified as water in the binary classification of the imagery. An overview of the underestimated areas for the four-gauge scenario developed with the 10-m DEM is shown in Figure 11. Furthermore, the mismatch in resolution between the Landsat imagery (at 30 m) and the 10-m and 1-m DEMs, given the unfortunate absence of other feasible satellite data sets, could have also influenced the error estimates in the accuracy assessment.

CONCLUSIONS

The study found that it is possible to create flood prediction maps with a reasonable level of accuracy using few data inputs. The largest total error percentage is less than 30 percent, and if the two–stream gauge case scenario was excluded, the largest total error percentage was only 23 percent. It is noteworthy that even though the errors may seem large, the study error percentages represent the least amount of data possible to create a flood hazard analysis map, based on DEMs and stream gauge water levels. Using this simple approach with projected peak stages will allow for accurate prediction of areas to be flooded, which can be considered a good first solution with which to start planning flood emergency management situations. The simplicity of this model makes it a useful asset in urban planning and future flood predictions, addressing the concerns presented by Al-Sabhan et al. (2003). For instance, if an area is expecting a flood of a certain intensity, all emergency planners need to do is to use a DEM and available data from stream gauges to simulate flood conditions.

Given access to minimal data, DEMs, and stream gauge data, the methods we present allow for quick, simple, and accurate vulnerability predictions. Furthermore, this simplified model is easier to implement by a wide range of staff and personnel, especially those who are not flood engineers. While the scenarios using the 30-m DEM resolutions or two-gauge scenarios were not optimal, they still produced results similar to the LiDAR-derived 10-m and 1-m resolution DEMs.

Using highly detailed data does not necessarily lead to better simulations or always produce better results; this was clearly shown by the accuracy assessment. Furthermore, the scenarios using the 1-m DEM also had a slightly larger total disagreement than did the 10-m DEM, which was unexpected. The computational difference between 30-m DEM use and 10-m DEM use is consistent with other hydrologic work (Jacoby et al., 2013). Schroeder et al. (2015) drew similar conclusions when developing stream profiles using 1-m and 10-m DEMs.

This study showed that higher stream gauge density (using more stream gauges) does not necessarily produce better results, as this statement was largely unsupported by our analysis. In fact, the four–stream gauge scenario has the highest overestimate and the lowest underestimate across all three DEM resolutions, as well as the least total error percentage. Regardless of the DEM resolution used, the four–stream gauge distribution has the best results based on total error (underestimation or overestimation). One or a combination of factors may have led to these results. The four-gauge scenario may have been an optimal distance between and/or spatial distribution of the gauges. Another possibility is that in the process of going from five- or six-gauge scenarios, a gauge with higher error may have been removed from the simulations. A future study may try different distributions and combinations than those used in the current study. This would further determine if accuracy is correlated to the location and distance between individual stream gauges.

ACKNOWLEDGMENTS

The authors acknowledge and thank two reviewers for their suggestions, which have improved the manuscript. The authors wish to thank King Abdulaziz University for the financial assistance afforded Anas Rabie while pursuing his M.S. degree.

REFERENCES

Akanbi, A. A. and Singh, K. P., 1997, *Managed Flood Storage Option for Selected Levees along the Lower Illinois River for Enhancing Flood Protection, Agriculture, Wetlands, and Recreation: Second Report, Validation of the UNET Model for the Lower Illinois River*: Illinois State Water Survey, Contract Report 608, 110 p.

Al-Sabhan, W.; Mulligan, M.; and Blackburn, G. A., 2003, A real-time hydrological model for flood prediction using GIS and the WWW: *Computers, Environment Urban Systems*, Vol. 27, No. 1, pp. 9–32, doi:10.1016/S0198-9715(01)00010-2.

Deng, Y.; Wilson, J. P.; and Gallant, J. C., 2008, Terrain analysis. In Wilson, J. P. and Fotheringham, A. S. (Editors), *The Handbook of Geographic Information Science*: Blackwell, Oxford, U.K., pp. 417–435.

El-Hames, A. S. and Richards, K. S., 1998, An integrated, physically based model for arid region flash flood prediction capable of simulating dynamic transmission loss: *Hydrological Processes*, Vol. 12, No. 8, pp. 1219–1232, doi:10.1002/(SICI)1099-1085(19980630)12:8<1219::AID-HYP613>3.0.CO;2-Q.

Fisher, P. F. and Tate, N. J., 2006, Causes and consequences of error in digital elevation models: *Progress Physical Geography*, Vol. 30, No. 4, pp. 467–489, doi:10.1191/0309133306pp492ra.

Galzki, J.; Mulla, D.; Joel, N.; and Wing, S., 2008, *Targeting Best Management Practices (BMPs) to Critical Portions of the Landscape: Using Selected Terrain Analysis Attributes to Identify High-Contributing Areas Relative to Nonpoint Source Pollution*: Minnesota Department of Agriculture.

Gesch, D. B., 2007, The national elevation dataset. In Maune, D. (Editor), *Digital Elevation Model Technologies and Applications: The DEM Users Manual*, 2nd ed.: American Society for Photogrammetry and Remote Sensing, Bethesda, MD, pp. 99–118.

Gesch, D. B., 2009, Analysis of Lidar elevation data for improved identification and delineation of lands vulnerable to sea-level rise: *Journal Coastal Research*, Special Issue 53. pp. 49–58, doi:10.2112/si53-006.1.

Gesch, D. B.; Oimoen, M.; Greenlee, S.; Nelson, C.; Steuck, M.; and Tyler, D., 2002, The national elevation dataset: *Photogrammetric Engineering Remote Sensing*, Vol. 68, No. 1, pp. 5–32.

Hammer, R. D.; Young, F. J.; Wollenhaupt, N. C.; Barney, T. L.; and Haithcoate, W., 1995, Slope class maps from soil survey and digital elevation models: *Soil Science Society America Journal*, Vol. 59, No. 2, pp. 509–519.

Jacoby, B.; Peterson, E. W.; Kostelnick, J. C.; and Dogwiler, T., 2013, Approaching cave level identification with GIS: A case study of Carter Caves: *ISRN Geology*, Vol. 2013, No. 160397, p. 7, doi:10.1155/2013/160397.

Kia, M.; Pirasteh, S.; Pradhan, B.; Mahmud, A.; Sulaiman, W.; and Moradi, A., 2012, An artificial neural network model for flood simulation using GIS: Johor River Basin, Malaysia: *Environmental Earth Sciences*, Vol. 67, No. 1, pp. 251–264, doi:10.1007/s12665-011-1504-z.

Kostelnick, J. C.; McDermott, D.; Rowley, R. J.; and Bunnyfield, N., 2013, A cartographic framework for visualizing risk: *Cartographica*, Vol. 48, No. 3, pp. 200–224, doi:10.3138/carto.48.3.1531.

Lian, Y; Chan, I.; Xie, H.; and Demissie, M., 2010, Improving HSPF modeling accuracy from FTABLES: Case study for the Illinois River Basin: *Journal Hydrologic Engineering*, Vol. 15, No. 8, pp. 642–650, doi:10.1061/(ASCE)HE.1943-5584.0000222.

Poulter, B. and Halpin, P. N., 2008, Raster modelling of coastal flooding from sea-level rise: *International Journal Geographical Information Science*, Vol. 22, No. 2, pp. 167–182, doi:10.1080/13658810701371858.

Rosner, A.; Vogel, R. M.; and Kirshen, P. H., 2014, A risk-based approach to flood management decisions in a nonstationary world: *Water Resources Research*, Vol. 50, No. 3, pp. 1928–1942, doi:10.1002/2013WR014561.

Safaripour, M.; Monavari, M.; Zare, M.; Abedi, Z.; and Gharagozlou, A., 2012, Flood risk assessment using GIS (case study: Golestan province, Iran): *Polish Journal Environmental Studies*, Vol. 21, No. 6, pp. 1817–1824.

Schroeder, K.; Peterson, E. W.; and Dogwiler, T., 2015, Field validation of DEM and GIS derived longitudinal stream profiles: *Journal Earth Science Research*, Vol. 3, No. 3, pp. 43–54, doi:10.18005/JESR0303002.

Watson, D. F. and Philip, G., 1985, A refinement of inverse distance weighted interpolation: *Geo-processing*, Vol. 2, No. 4, pp. 315–327.

Worthen, A. H., 1868, *Geology of Illinois*: Legislature of Illinois.

Zhang, X.; Drake, N. A.; Wainwright, J.; and Mulligan, M., 1999, Comparison of slope estimates from low resolution DEMS: Scaling issues and a fractal method for their solution: *Earth Surface Processes Landforms*, Vol. 24, pp. 763–779.